



Study and effect of GTAW parameters on mechanical properties of aluminium dissimilar welded joints: optimization technique

Abhishek Saxena^{1,2} · Kuldeep K. Saxena³ · Bharat Singh¹ · S. K. Rajput⁴ · Balram Yelamasetti⁵

Received: 21 March 2023 / Accepted: 23 November 2023

© The Author(s), under exclusive licence to Springer-Verlag France SAS, part of Springer Nature 2023

Abstract

In this research, dissimilar metals of AA 6082 and AA 7075 are joined using Gas Tungsten Arc Welding (GTAW) process with ER4043 filler wire. The welding conditions and their range are identified for producing quality welding characteristics. Taguchi based techniques are adopted for design of experimentation and analyzing factors involved in welding characteristics. L-9 Orthogonal Array (OA) was used for Design of Experiments (DOE). Welding current, filler diameter and root gaps are selected as input parameters. The welded structure defects were inspected with X-ray radiography images as well as macrostructures. The response factors such as Ultimate Tensile Strength (UTS), % of elongation, hardness and impact strength were considered and evaluated by conducting mechanical tests. Analysis of Variance (ANOVA) is conducted to study the influence of parameters on responses. The tensile strength of sample 5 is increased by 53.37% when compared with the sample 6 due to the lower heat input rates. The welding speed (68%) has most influence parameter followed by welding current (14%) and filler diameter (14%). The dissimilar combination of aforementioned joints have wide range of application including aerospace, defense, and military sectors.

Keywords AA6082 · AA7075 · GTAW · Taguchi methods · ANOVA · Mechanical properties

1 Introduction

Fusion welding technique is one of primary manufacturing processes for joining of similar metals and dissimilar metals to obtain monolithic structures. [1, 2]. During joining of dissimilar metals, suitable welding technique and filler wire play a vital role for producing sound welded structures. Joining of dissimilar metals using fusion welding process is challenging and difficult to achieve desired welding properties than

similar weldments because of differences in chemical compositions, phase structures and their mechanical and thermal properties [3, 4]. Mohd et al. [5] compared the laser-MIG and Tungsten Inert Gas (TIG) welding processes for joining the Inconel materials of 10 mm thickness. Micro and nano-indentations were made on weld samples to measure the hardness at different zones. The bead structures were studied using different techniques (optical and scanning electron microscope). Higher weld strength was observed when the samples were joined using laser welding process than the TIG welding process. Also, it reduces the distortion effect and weld bead to width ratio when laser welding process is used. Xiaogang et al. [6] reported the high temperature fracture of NG-TIG welding samples of Inconel material. Twin grain boundaries with less distortion were identified at the interface of weld zone which could be attributed to improve of toughness [7]. Mabuwa et al. [8, 9] developed the Al dissimilar joints using FSP + TIG processes to study the metallurgical changes in the nugget zone and report that the intermetallic compounds were observed in the nugget zone when low rotational speed is maintained. Higher hardness number was observed when both the welding processes employed. The stresses developed in the dissimilar weldments of AA6061

✉ Balram Yelamasetti
Balram3072@gmail.com

¹ Department of Mechanical Engineering, GLA University, Mathura 281406, India

² Department of Mechanical Engineering, ABES Engineering College, Ghaziabad, UP 201009, India

³ Division of Research and Development, Lovely Professional University, Phagwara 144411, India

⁴ Department of Mechanical Engineering, BIET, Jhansi 284001, India

⁵ Department of Mechanical Engineering, MLR Institute of Technology, Hyderabad, Telangana 500043, India

and AA7075 also reduced when combination of FSP and TIG welding is employed [10].

Aluminum 6XXX and 7XXX alloys are widely used in the aerospace industry, food technologies and automobile industries. The corrosion resistance of these alloys are particularly good enough when compared with other Al alloys [11]. Different types of Aluminum alloy series are developed for industrial applications due to low density weight ratio and high strength [12, 13]. Aluminum alloy 6XXX is a precipitation-hardened Al alloy which contains Mg and Si as its main elements. AA7075 is Zinc based alloy which is mostly used for aircraft industries. The major alloying elements contains in this material is Zn of 5.62%, Mg of 2.32% and Cu of 1.28%. By adding zinc alloying element to Al metals which controls the grain structure resulting in improving strength of alloy [14, 15]. Aluminum Alloy 7075 is a high strength possesses good resistance against corrosion environment and is the most commonly used alloy for machining. Bajpei et al. [16, 17] developed the Al dissimilar joint using MIG welding process by changing different welding current and heat input rates. The welded plates have more stable by fixing clamping at the edges in order to reduce distortion effect. Balram et al. [18–20] developed the dissimilar welded joint using fusion welding process and Friction Stir Welding (FSW) process. The process parameters have been fixed by performing trail experiments and design of experiments. The better properties were identified when the samples were joined using TIG welding process than the FSW process. Also, the grain structure and uniform distribution are observed in the interface and Heat Affected Zone (HAZ). During the welding, the current is considered as the main parameter to determine the welding characteristics and heat input. The grain boundaries growth and sub-structures were observed during pulse current mode when main current is increased [21, 22].

The similar and dissimilar combination of Al series were joined using FSW, MIG and TIG welding processes to study the weldability, welding characteristics, stress development and metallurgical studies. Also, the effect of FSW parameters on the Al welded structures are reported. Producing of quality welded structures using fusion welding techniques and homogeneity in the structures is the challenge. The effect of process parameters of GTAW on welding characteristics of dissimilar combination of AA6082 and AA7075 is studied in this research. This combination of Al plates are having wide

range of application in many sectors including aerospace, automobile and food technologies which are used for producing good strength and corrosion resistance. Parameters used in this study and their effects on weld strength and metallurgical properties are reported.

2 Materials and experimentation

The base metals, AA6082 and AA7075, are sliced using WEDM process with the specimen dimension of $150 \times 100 \times 5$ mm. The each specimen is made groove configuration at the corner with included angle of 30° to fill the material (ER4043). Butt joint groove configuration is made with land of 1.5 mm. The base specimen edges are cleaned with rotary wire brush to remove the blur particles. Clamping is made on two specimens by keeping root gap of 2 mm to fix the specimen position. Argon gas flow rate is maintained in each pass to shield the weld pool from other gases. In this research, LINCOLN 375 welding machine is used. The composition (wt.%) of parent metals and filler are listed in Table 1. The flow chart of present research work is mentioned in Fig. 1. The parameters (current, filler diameter and torch speed) and their range are listed in Table 2. Taguchi based L-9 OA is used for DOE and the same is mentioned in Table 3. The developed welded structures according to DOE are shown in Fig. 2. The welded samples were sliced for various testing's as per standards using WEDM process and the sliced test specimens are shown in Fig. 3. The mechanical properties of dissimilar welded joints were evaluated by conducting tensile test on UTM, impact energy on IZOD test and hardness measurement using Brinell hardness tester. The tensile test samples were sliced and tested as per the ASTM E/8 standards with a shear rate of 2 mm/min. The weld surfaces were cleaned using velvet cloth by applying emery sheets with different grit sizes to capture the micro/macrographs using optical microscope.

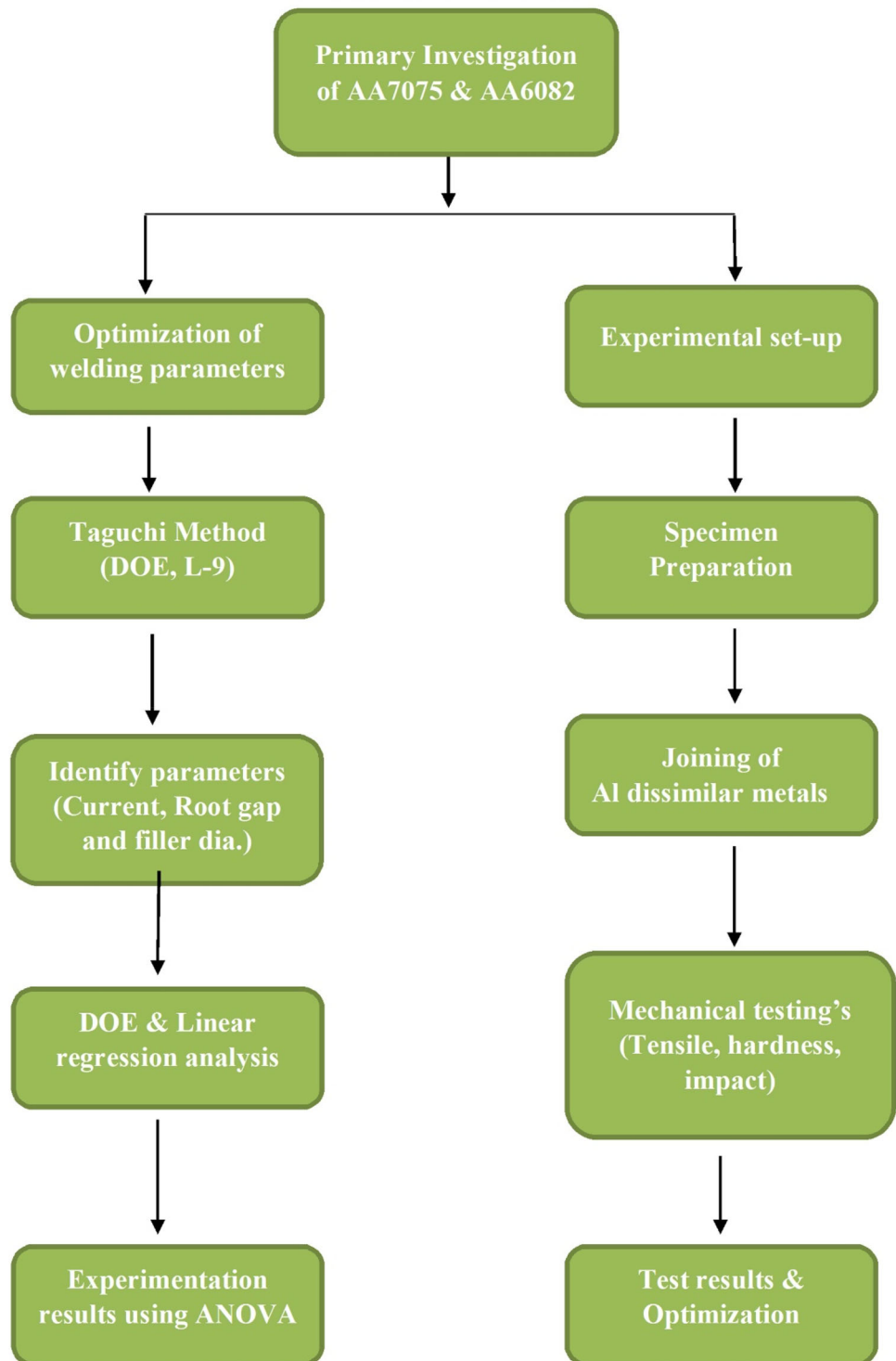
3 Results & discussions

3.1 Mechanical behaviour

The tensile test specimens were tested on UTM machine with constant shear rate. It is clearly observed that all the tensile

Table 1 Composition of base/filler metals [13]

Base/filler metals	Al	Mg	Zn	Cr	Mn	Si	Cu	Fe
AA6082	Bal	1.2	0.09	0.25	0.8	0.8	0.09	0.5
AA7075	Bal	2.8	5.9	0.19	0.02	0.06	1.91	0.14
ER4043	Bal	0.09	0.1	-	0.05	4.58	0.3	0.8

Fig. 1 Methodology of research work

samples were fractured at the interface of AA6082. The weld properties from the tensile test are shown in Table 4. From the test results, the maximum UTS of 227 MPa is observed for sample 5 when the filler diameter at 3.2 mm and torch speed at 45 mm/min were maintained. Whereas lower UTS of 148 MPa is observed for sample 6 when the filler diameter

at 1.6 mm and torch speed at 60 mm/min were maintained. Higher weld strength was observed when higher filler diameter is maintained whereas lower UTS values was observed with less filler diameter and higher welding speed. The dissimilar weldments of Al alloys are exhibiting better tensile properties when welding current of 100 A and welding torch

Table 2 Parameters used and levels

Parameters/levels	Low	Medium	High
welding current, A	100	105	110
Filler dia., mm	1.6	2.4	3.2
Torch speed, mm/min	30	45	60

Table 3 Orthogonal array used for welding process

Exp. no	Dia. of filler (mm)	Weld current (A)	Welding speed, (mm/s)
1	Ø1.6	100	30
2	Ø2.4	100	45
3	Ø3.2	100	60
4	Ø2.4	105	30
5	Ø3.2	105	45
6	Ø1.6	105	60
7	Ø3.2	110	30
8	Ø1.6	110	45
9	Ø2.4	110	60

speed of 45 mm/min were maintained. The tensile strength of sample 5 is increased by 53.37% when compared with the sample 6.

The toughness of the welded samples were tested with IZOD testing machine as per the standards and the obtained results are listed in Table 4. Under the impact loads, the welded samples were observed strain energy before fracture. The maximum toughness value (3.3 J/mm²) was witnessed at test trail number 8 and lower energy value (2.4 J/mm²) was witnessed at test trail number 3. The better impact strength values are perceived when the current is high and lower energy values were perceived when the higher torch speeds were maintained. The toughness of sample 8 was improved by 37.5% when compared with sample 3.

The surface hardness number of dissimilar welded joints were measured using Brinell tester along the weld line by considering suitable indenter. The average value at weld zone of nine welded samples are listed in Table 4. The maximum hardness of 114 BHN for sample 3 and minimum hardness of 96 BHN for sample 5 were observed. The higher hardness number is observed when the welding current is lower with high welding speed were maintained whereas, the lower hardness number was observed when 3.2 mm filler diameter used. Due to the more heat input especially at higher currents, the welded samples exhibited minimum surface hardness which resulted in lower UTS. This could be reasoned by forming lower grain size and recrystallization phases [23]. The welded structures with higher filler diameter exhibited

higher hardness number due to the required filament addition at the fusion zone.

3.2 Optimization process

Analysis of Variance has been performed for each responses and studied the effect of each welding parameter on response factors [24]. ANOVA was performed for UTS, hardness number and toughness of dissimilar weldments. This process is carried out using statistical tool Minitab application. To measure the total mean for the responses the following Eq. (1) is used. This equation will find the sum of squared deviations and this will be converted in two part using Eq. 2. The sum of the squared deviation is calculated using Eq. 3. The design parameters and contribution percentages are calculated using Eq. 4.

$$SS_T = \sum_{j=1}^n (\gamma_j - \gamma_m) \quad (1)$$

$$SS_T = \sum_{j=1}^{n_p} SS_j + SS_e \quad (2)$$

$$SS_j = \sum_{i=1}^l (n_{ij} - \gamma_m)^2 \quad (3)$$

$$\beta_j = \frac{SS_j}{SS_T} \quad (4)$$

The effect of welding parameters on response factors are calculated and shown in Table 5. The welding speed has great significance on the responses followed with other parameters (welding current and filler diameter). The higher the speed lower the heat input which will enhance the welding characteristics. The welding speed has 68% contribution for improving the welding strength. The filler wire has 14% contribution for developing bead height with less segregation effect due to filler alloying elements [25]. The residual plots of each response factors are shown in Figs. 4, 5, and 6. It is evident that the residuals of tensile strength, hardness and impact strength are normally distributed with very little deviation (Figs. 4a, 5a, and 6a). Also the residuals do not have any particular shape and are randomly scattered from zero (Figs. 4b, 5b, and 6b). The frequency of residuals of the values is also shown in bar chart (Figs. 4c, 5c, and 6c) There is no time tendency along with drift in the model towards lower number values was observed as apparent from Residual vs. observation order plot (Figs. 4d, 5d, and 6d).

3.3 Microstructural studies

The microstructure of base metals and welded joints were captured using optical microscope after smooth polishing of

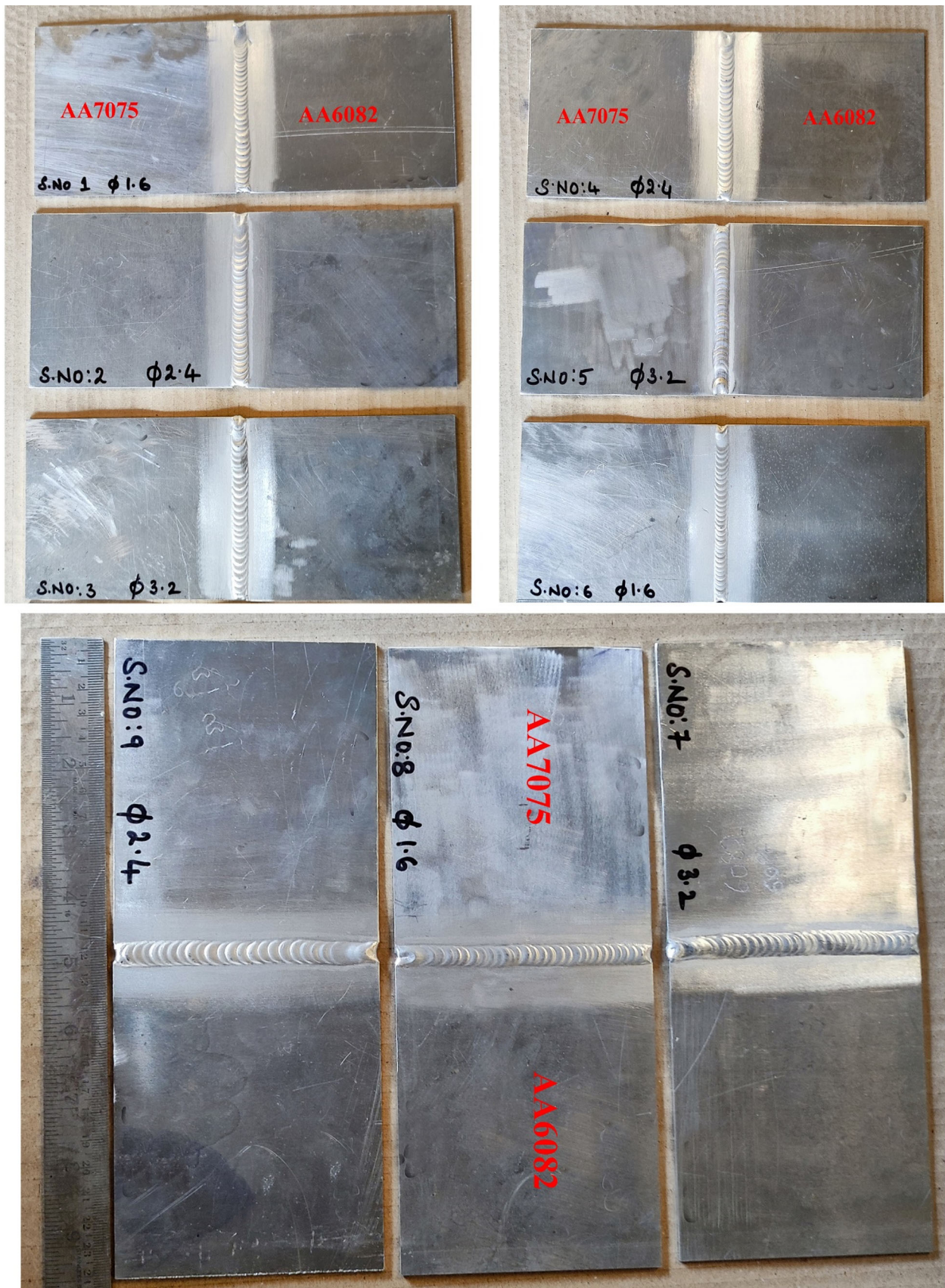
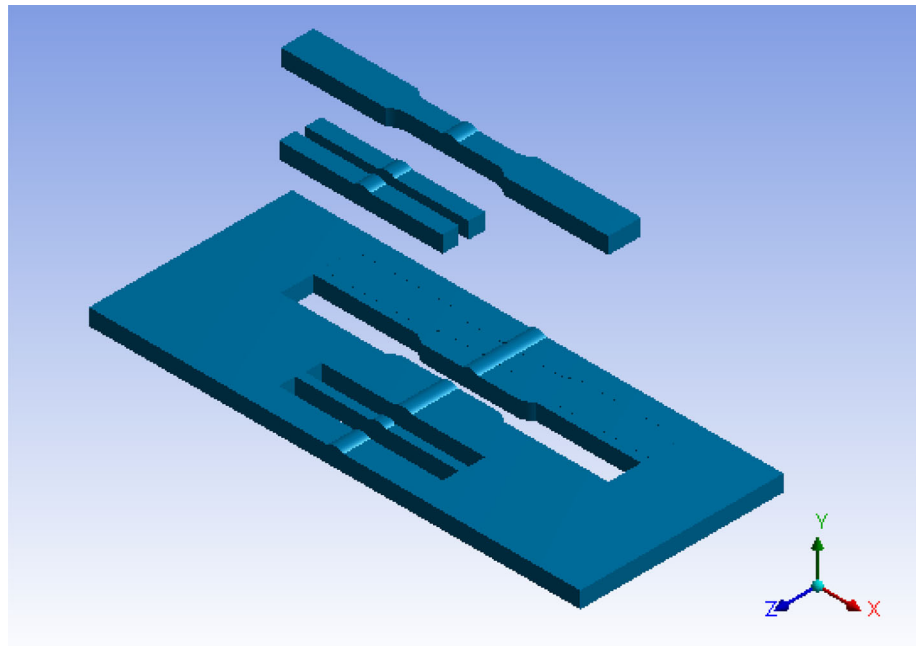


Fig. 2 Developed joints using GTAW process

Fig. 3 Welding coupons for testing**Table 4** Parameters and their mechanical properties

Exp. no	Electrode work piece Distance (mm)	Argon Gas flow rate (l/min)	Welding speed (mm/s)	Current (A)	UTS, MPa	Impact energy (J/mm ²)	Average hardness value
1	Ø1.6	4–8	30	95	183	3	107
2	Ø2.4	4–8	45	95	200	3	108
3	Ø3.2	4–8	60	95	162	2.4	114
4	Ø2.4	4–8	30	100	181	3	112
5	Ø3.2	4–8	45	100	227	2.5	96
6	Ø1.6	4–8	60	100	148	3	103
7	Ø3.2	4–8	30	105	184	3	105
8	Ø1.6	4–8	45	105	187	3.2	106
9	Ø2.4	4–8	60	105	192	2.5	104

Table 5 ANOVA results for output responses

Source	DF	Adj. SS	Adj. MS	% of contribution	Significant
Welding current	2	0.082	0.041	14%	Less significant
Filler dia	2	0.082	0.041	14%	Less significant
Welding speed	2	0.389	0.194	68%	More significant
Error	2	0.016	0.008	4%	–
Total	8	0.569			

specimens. The microstructures were captured at different locations for the optimum welded sample (welding current at 100 A, welding speed at 60 mm/min). The base metals microstructures are shown in Fig. 7. The Si and Mg alloying elements existed in major portion in AA6082 (shown in Fig. 7b) whereas Zn and Mg alloying elements are clearly

shown in Fig. 7a. The microstructures of welded samples are captured at different locations are shown in Fig. 8. The fusion zone of welded joint at top and bottom zones are shown in Fig. 8a, b. It is clearly observed that the welded structures have uniform filler wire distribution with exi-axis

Residual Plots for Tensile strength (MPa)

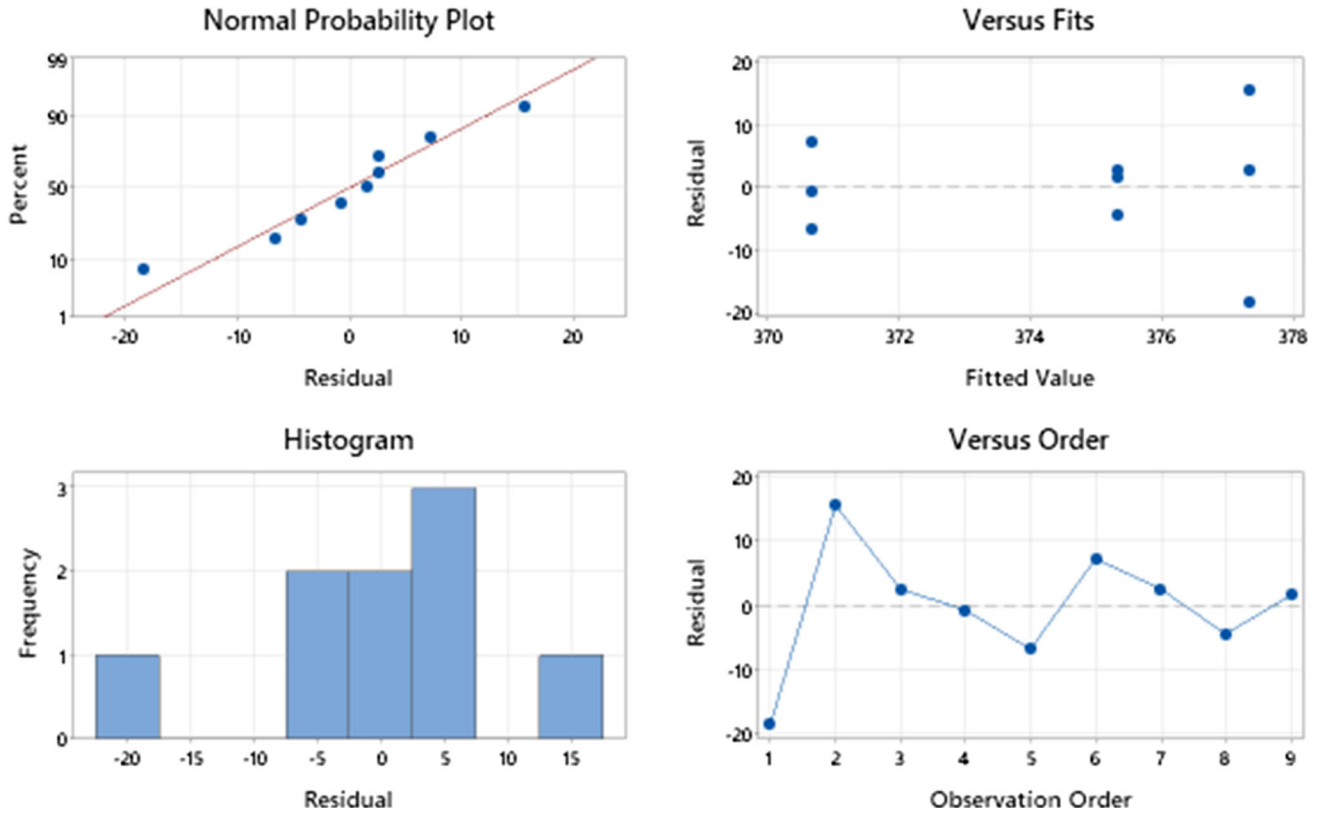


Fig. 4 Residual plot for UTS

Residual Plots for Hardness (BHN)

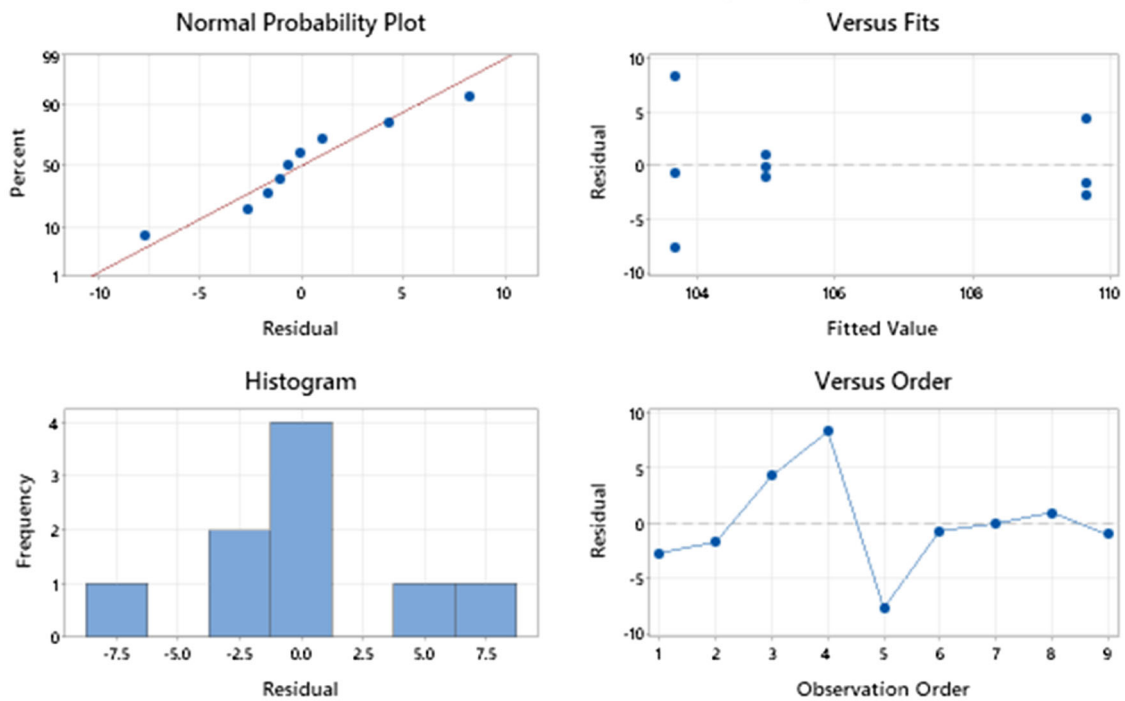


Fig. 5 Residual plot for Hardness

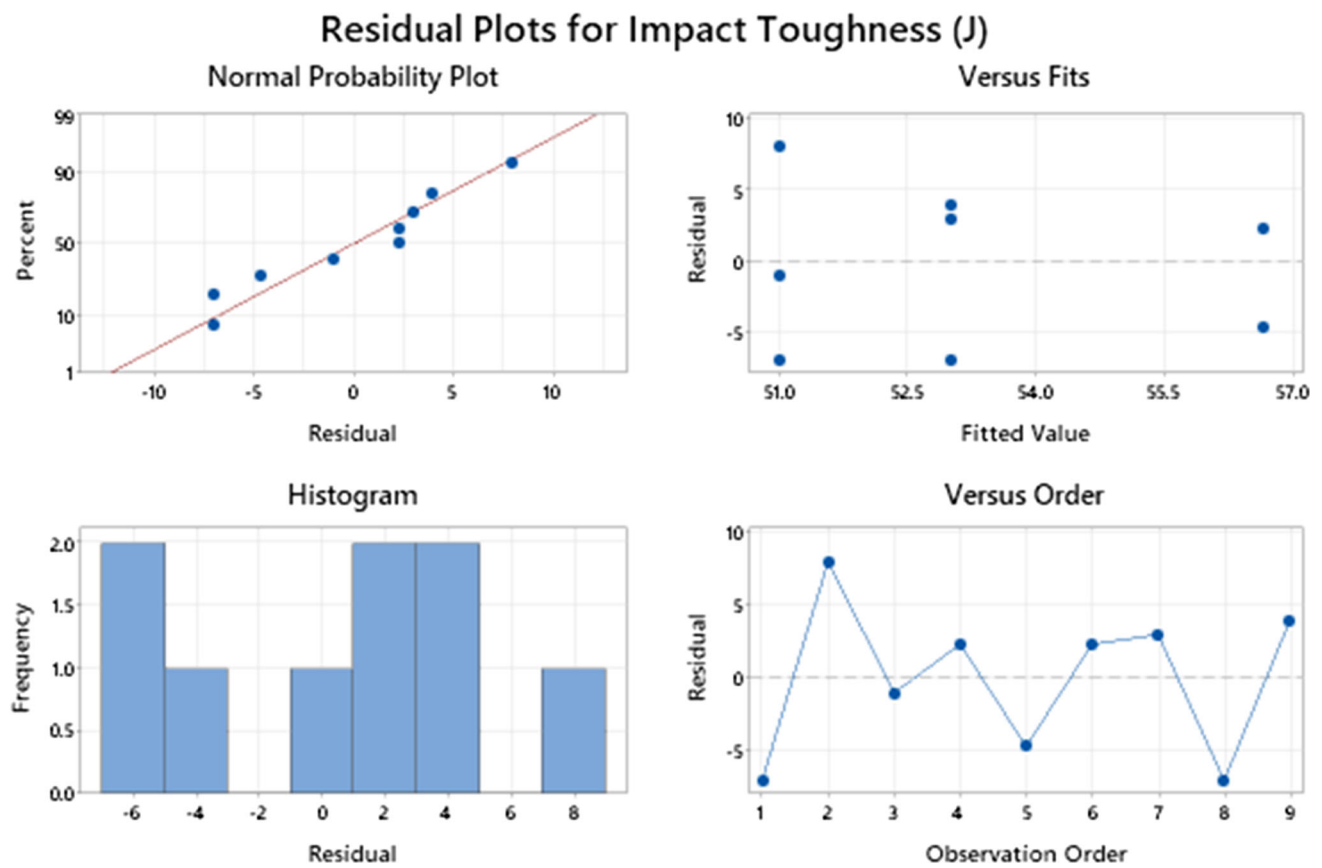


Fig. 6 Residual plot for Toughness

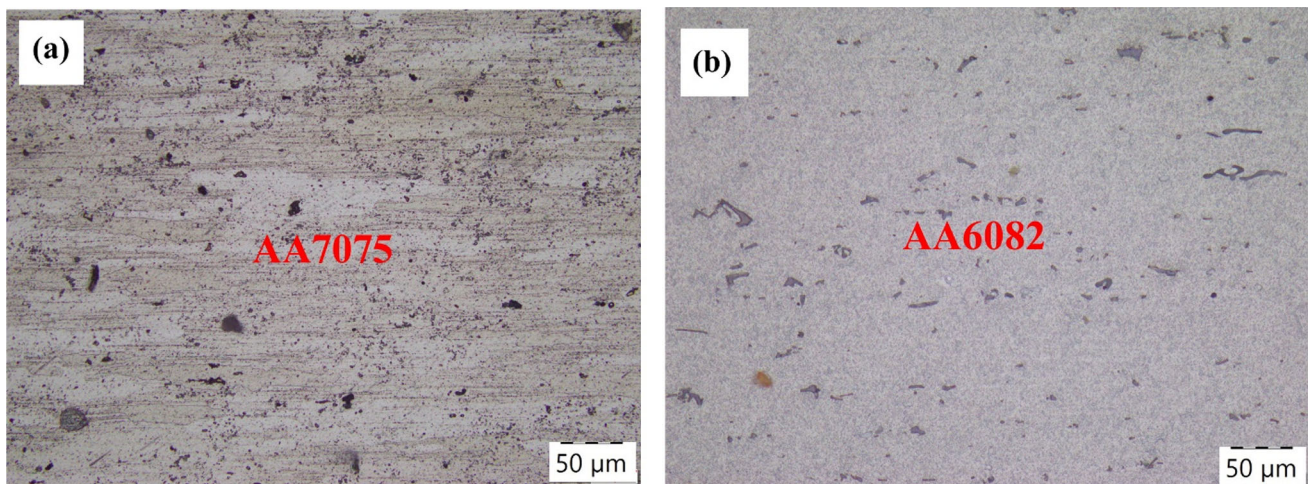


Fig. 7 Microstructure of base metals a AA7075, b AA6082

cellular grain structures. The weld bottom zone has fine structure with clear grain boundaries. Fine grains with equiaxed particles evenly distributed in the weld region have been observed which led to producing defect-free weld joints [26, 27]. Also which could be attributed to enhance the welded structures properties in-terms of UTS and higher hardness

values. A similar structural properties were identified in Al alloys welded samples [28, 29]. The HAZ of welded structures are shown in Fig. 8c, d. The low amount of alloying elements (Zn, Mg) segregation were identified at the interface of AA7075 whereas the segregation of filler alloying elements can be clearly seen at the HAZ of AA6082 which

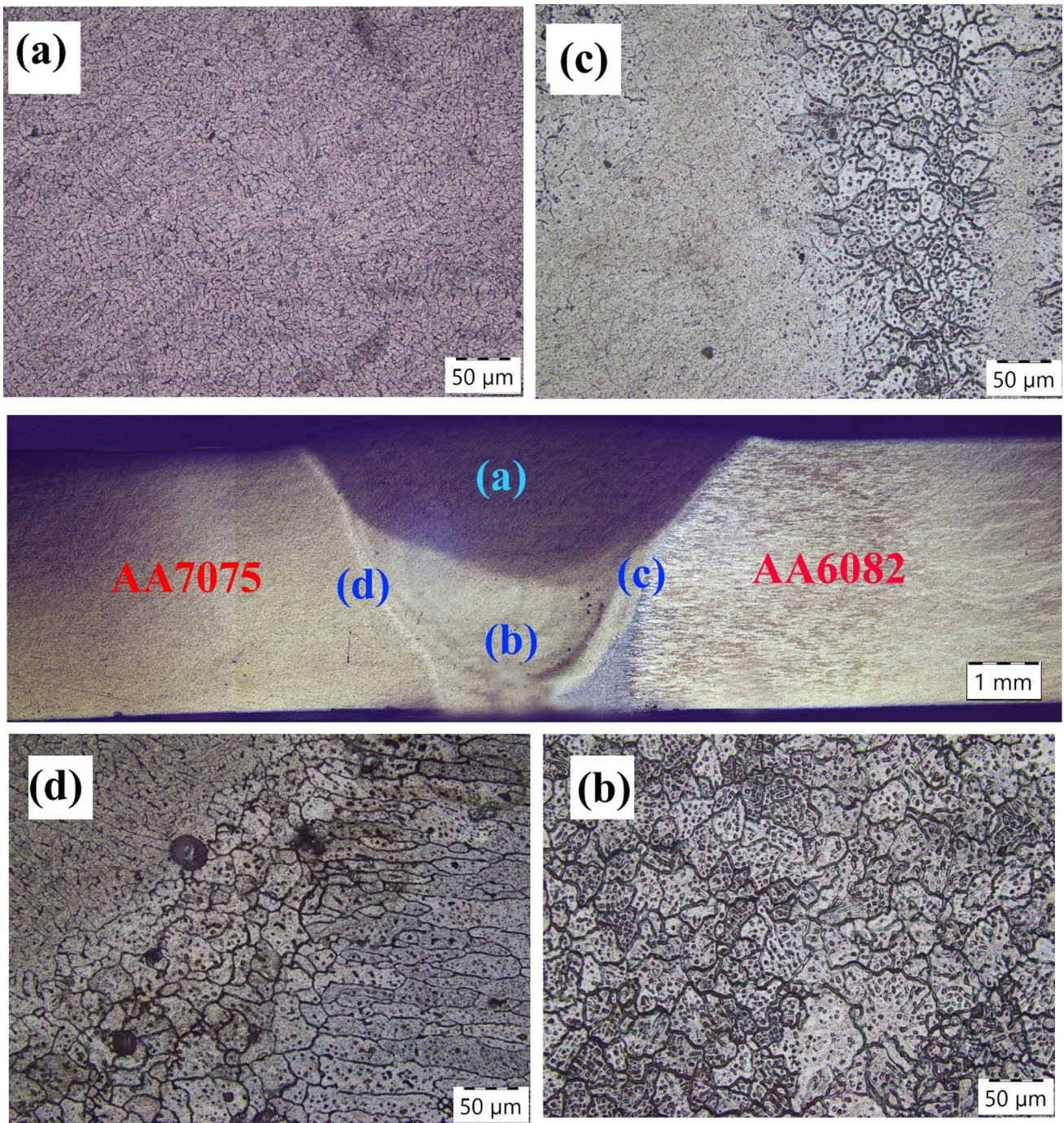


Fig. 8 Microstructure of dissimilar welded joint **a, b** weld zone, **c, d** HAZ of AA6082 and AA7075

led to fracture under tensile loading condition. The weld roots possess good strength due to the TIG welding technique and which may exhibits higher corrosion resistance especially at the weld root. The grain structures near the AA7075 interface were found uniform distribution over the weld bead.

4 Conclusions

The following conclusions are drawn from the experimentation, testing and optimization analysis;

- The dissimilar weldments of AA6083 and AA7075 were successfully developed by employing GTAW process using ER4043 as filler rod.

- The experimentation process has been carried out successfully according to factorial method to analyze the various parameters.
- The maximum UTS value was observed when welding current of 100 A, filler diameter of 3.2 mm are used. The tensile strength of sample 5 is increased by 53.37% when compared with the sample 6 due to the lower heat input rates.
- The maximum hardness number was observed when the lower welding current (95 A) and higher welding speed (75 mm/min) were maintained. Whereas, the lower hardness number was observed when 3.2 mm filler diameter is used.
- The better toughness values were identified when the welding current is maintained at high level whereas low toughness values were observed with the lower welding speed.
- From ANOVA, the welding speed is main influencing parameter for better strength, hardness and toughness of dissimilar weldments of AA6082 and AA7075. The welding speed has great significance (68%) on the responses followed with other parameters.
- Fine grains with equi-axed particles were observed which led to producing defect-free welded joints. Due to the continuous heat input to the base metals, slight segregation effect can be seen at the interface of AA6062.

Data availability Data is contained within the article.

Declarations

Conflict of interest The authors declare no conflict of interest.

References

1. Qin, Q., Zhao, H., Li, J., et al.: Microstructures and mechanical properties of TIG welded Al-Mg₂Si alloy joints. *J. Manuf. Process.* **56**, 941–949 (2020). <https://doi.org/10.1016/j.jmapro.2020.05.058>
2. Padmanaban, G., Balasubramanian, V.: Influences of pulsed current parameters on mechanical and metallurgical properties of gas tungsten arc welded AZ31B magnesium alloys. *Met. Mater. Int.* **17**, 831–839 (2011). <https://doi.org/10.1007/s12540-011-1022-2>
3. Yelamasetti, B., Rajyalakshmi, G.: Residual stress analysis, mechanical and metallurgical properties of dissimilar weldments of Monel 400 and AISI 316. *Int. J. Mater. Res.* **111**, 880–893 (2020). <https://doi.org/10.1515/ijmr-2020-1111102>
4. Arun, D., Ramkumar, K.D., Vimala, R.: Multi-pass arc welding techniques of 12 mm thick super-duplex stainless steel. *J Mater Proc Technol* **271**, 126–143 (2019)
5. Aqeel, M., Gautam, J.P., Shariff, S.M.: Comparative study on auto-genous diode laser, CO₂ laser-MIG hybrid and multi-pass TIG welding of 10-mm thick Inconel 617 superalloy. *Mater. Sci. Eng. A* **856**, 143967 (2022). <https://doi.org/10.1016/j.msea.2022.143967>
6. Li, X., Li, K., Li, S., Yao, Wu., Cai, Z., Pan, J.: Microstructure and high temperature fracture toughness of NG-TIG welded Inconel 617B superalloy. *J. Mater. Sci. Technol.* **39**, 173–182 (2020). <https://doi.org/10.1016/j.jmst.2019.07.021>
7. Eghlimi, A., Shamanian, M., Eskandarian, M., Zabolian, A., Szpunar, J.A.: Characterization of microstructure and texture across dissimilar super duplex/austenitic stainless steel weldment joint by austenitic filler metal. *Mater Charact* **106**, 208–217 (2015)
8. Mabuwa, S., Msomi, V., Mehdi, H., Ngonda, T.: A study on the metallurgical characterisation of the longitudinally sampled friction stir processed TIG welded dissimilar aluminum joints. *Proc Inst Mech Eng, Part E: J Proc Mech Eng* (2023). <https://doi.org/10.1177/09544089231169589>
9. Mabuwa, S., Msomi, V., Mehdi, H., Saxena, K.K.: Effect of material positioning on Si-rich TIG welded joints of AA6082 and AA8011 by friction stir processing. *J. Adhes. Sci. Technol.* **37**(17), 2484–2502 (2023). <https://doi.org/10.1080/01694243.2022.2142366>
10. Mehdi, H., Mishra, R.S.: Influence of friction stir processing on weld temperature distribution and mechanical properties of TIG-welded joint of AA6061 and AA7075. *Trans. Indian Inst. Met.* **73**, 1773–1788 (2020). <https://doi.org/10.1007/s12666-020-01994-w>
11. Yadav, A.K., Agrawal, M.K., Saxena, K.K., et al.: Numerical simulation and experimental residual stress analyses of dissimilar GTA weldments of AA 5083 and AA 6082. *Int. J. Interact. Des. Manuf.* (2023). <https://doi.org/10.1007/s12008-023-01216-9>
12. Balram Yelamasetti, P., Kumar, N., Venkat Ramana, G., Saxena, K.K., Singh, D., Kang, A.S., Mohammed, K.A.: Wear and corrosion behaviour of multiple pass friction stir processing on aluminium alloy 6061 embedding with B4C particles. *Adv Mater Proc Technol* (2023). <https://doi.org/10.1080/2374068X.2023.2171667>
13. Yelamasetti, B., G VR, Manikyam S, Saxena KK.: Multi-response Taguchi grey relational analysis of mechanical properties and weld bead dimensions of dissimilar joint of AA6082 and AA7075. *Adv Mater Process Technol* **00**, 1–11 (2021). <https://doi.org/10.1080/2374068x.2021.1946340>
14. Kumar, R., Kumar, G., Roy, A., et al.: A comparative analysis of friction stir and tungsten inert gas dissimilar AA5082-AA7075 butt welds. *Mater Sci Energy Technol* **5**, 74–80 (2022). <https://doi.org/10.1016/j.mset.2021.12.002>
15. Venkat Ramana, G., Yelamasetti, B., Vishnu Vardhan, T.: Study on weldability and effect of post heat treatment on mechanical and metallurgical properties of dissimilar AA 2025, AA 5083 and AA7075 GTAW weld joints. *Mater Today Proc* **46**, 878–882 (2021). <https://doi.org/10.1016/j.matpr.2020.12.1115>
16. Tapas Bajpei, H., Chelladurai, M.Z., Ansari.: Experimental investigation and numerical analyses of residual stresses and distortions in GMA welding of thin dissimilar AA5052-AA6061 plates. *J. Manuf. Process.* **25**, 340–350 (2017). <https://doi.org/10.1016/j.jmapro.2016.12.017>
17. Bajpei, T., Chelladurai, H., Ansari, M.Z.: Mitigation of residual stresses and distortions in thin aluminium alloy GMAW plates using different heat sink models. *J. Manuf. Process.* **22**, 199–210 (2016). <https://doi.org/10.1016/j.jmapro.2016.03.011>
18. Venkat Ramana, G., Yelamasetti, B., Vishnu Vardhan, T.: Effect of FSW process parameters and tool profile on mechanical properties of AA 5082 and AA 6061 welds. *Mater Today Proc* (2021). <https://doi.org/10.1016/j.matpr.2020.12.801>
19. Yelamasetti, B., Kumar, P.N., Venkat Ramana, G., et al.: Surface modification of aluminum alloy 6061 by embedding B4C particles via friction stir processing. *Mater Res Express* (2022). <https://doi.org/10.1088/2053-1591/ac6da7>
20. Yelamasetti, B., Vardhan, T.V., Ramana, G.V.: Study of metallurgical changes and mechanical properties of dissimilar weldments developed by interpulse current TIG welding technique. *Proc. Inst. Mech. Eng. C J. Mech. Eng. Sci.* **235**(16), 2985–2997 (2021). <https://doi.org/10.1177/0954406220960780>

21. Yelamasetti, B., G R, G VR, et al.: Comparison of metallurgical and mechanical properties of dissimilar joint of AISI 316 and Monel 400 developed by pulsed and constant current gas tungsten arc welding processes. *Int. J. Adv. Manuf. Technol.* **108**, 2633–2644 (2020). <https://doi.org/10.1007/s00170-020-05562-w>
22. Sen, R., Choudhury, S.P., Kumar, R., Panda, A.: A comprehensive review on the feasibility study of metal inert gas welding. *Mater Today: Proc* **5**(9), 17792–17801 (2018). <https://doi.org/10.1016/j.matpr.2018.06.104>
23. Yelamasetti, B., Rajyalakshmi, G., Sravan Kumar, K.: Mechanical and microstructural studies of optimized taguchi grey relational analysis of pcgtaw process parameters for joining monel 400 and AISI 316. *UPB Sci Bull Ser B Chem Mater Sci* **83**, 253–264 (2021)
24. Kumar, G.V., Gopalakrishnaiah, P., Devi, M.R., et al.: Multi parameter optimization in end milling of S-glass fiber reinforced polymer composite using Taguchi technique coupled with grey relational analysis. *Int. J. Interact. Des. Manuf.* (2023). <https://doi.org/10.1007/s12008-023-01274-z>
25. Roy, A., Ghosh, N., Mondal, S.: Effect of heat input on mechanical and metallurgical properties of AISI 304L stainless steel by using TIG welding. *Weld. Int.* **37**(2), 91–100 (2023). <https://doi.org/10.1080/09507116.2023.2185169>
26. Mehdi, H., Jain, S., Msomi, V., et al.: Effect of intermetallic compounds on mechanical and microstructural properties of dissimilar alloys Al-7Si/AZ91D. *J. Materi Eng and Perform* (2023). <https://doi.org/10.1007/s11665-023-08302-9>
27. Jain, S., Mishra, R.S., Mehdi, H.: Influence of SiC microparticles and multi-pass FSW on weld quality of the AA6082 and AA5083 dissimilar joints. *SILICON* (2023). <https://doi.org/10.1007/s12633-023-02455-x>
28. Yadav, A.K., Agrawal, M.K., Saxena, K.K., et al.: Effect of GTAW process parameters on weld characteristics and microstructural studies of dissimilar welded joints of AA5083 and AA6082: optimization technique. *Int. J. Interact. Des. Manuf.* (2023). <https://doi.org/10.1007/s12008-023-01230-x>
29. Vetrivel Sezhian, M., Giridharan, K., Peter Pushpanathan, D., Chakravarthi, G., Stalin, B., Karthick, A., Bharani, M.: Microstructural and mechanical behaviors of friction stir welded dissimilar AA6082-AA7075 joints. *Adv. Mater. Sci. Eng.* **2021**, 1–13 (2021). <https://doi.org/10.1155/2021/4113895>

Publisher's Note Springer Nature remains neutral with regard to jurisdictional claims in published maps and institutional affiliations.

Springer Nature or its licensor (e.g. a society or other partner) holds exclusive rights to this article under a publishing agreement with the author(s) or other rightsholder(s); author self-archiving of the accepted manuscript version of this article is solely governed by the terms of such publishing agreement and applicable law.